

## **A MINIATURIZED PRINTED DIPOLE ANTENNA WITH V-SHAPED GROUND FOR 2.45 GHZ RFID READERS**

**Z. G. Fan, S. Qiao, J. T. Huangfu, and L. X. Ran** <sup>†</sup>

Department of Information and Electronic Engineering  
Zhejiang University  
Hangzhou 310027, China

**Abstract**—In this paper, a miniaturized printed dipole antenna with the V-shaped ground is proposed for radio frequency identification (RFID) readers operating at the frequency of 2.45 GHz. The principles of the microstrip balun and the printed dipole are analyzed and design considerations are formulated. Through extending and shaping the ground to reduce the coupling between the balun and the dipole, the antenna's impedance bandwidth is broadened and the antenna's radiation pattern is improved. The 3D finite difference time domain (FDTD) Electromagnetic simulations are carried out to evaluate the antenna's performance. The effects of the extending angle and the position of the ground are investigated to obtain the optimized parameters. The antenna was fabricated and measured in a microwave anechoic chamber. The results show that the proposed antenna achieves a broader impedance bandwidth, a higher forward radiation gain and a stronger suppression to backward radiation compared with the one without such a ground.

### **1. INTRODUCTION**

Dipole antennas are extensively utilized in varieties of applications such as being the basic units of phased-array antennas and the feeding sources of aperture antennas [1–3]. Compared with traditional line antennas, printed dipole antennas have extra advantages including planar structure, small volume, light weight and low cost, which are significantly suitable for applications sensitive to the receiver sizes.

---

<sup>†</sup> The second author is also with Zhejiang University City College, Hangzhou 310025, China. The third and fourth authors are also with The Electromagnetics Academy at Zhejiang University, Zhejiang University, Hangzhou 310027, China.

A standard dipole antenna has an omni-directional radiation pattern. However, in modern wireless communication systems, directive gains are frequently needed or required, for example, for cell phones, mobile base stations and long range RFID readers [4]. In addition, with the development of broadband wireless communications, a printed antenna with broad operational bandwidth is also preferred in many wireless applications, for example, the ultra-wideband (UWB) radios [5]. However, a printed dipole antenna inherently operates in a narrow frequency band, which is the shortcoming needed to be overcome before its advantages can be used in aforementioned applications.

In this paper, based on the early researches [6, 7], we propose a novel miniaturized printed dipole antenna for 2.45 GHz RFID readers, which achieves simultaneously broad bandwidth and high directivity gain through introducing a V-shaped ground to the traditional printed dipole antenna. The paper is organized as following: firstly, the principles of the microstrip balun and the printed dipole are analyzed and formulated. Then, in order to broaden the impedance bandwidth, we extend and shape the antenna's ground to reduce the coupling between the balun and the dipole, which also improves the radiation patterns. A three-dimensional (3D) finite difference time domain (FDTD) electromagnetic simulations are carried out to evaluate the antenna performance, and to obtain the optimized design parameters by varying the extending angle and the position of the ground in the simulation. Finally, we fabricated the antenna and measured it in a microwave anechoic chamber. The experimental results show that the proposed printed antenna is indeed with broader impedance bandwidth, higher forward radiation gain and larger suppression to backward radiation than a traditional one without such a ground.

## 2. DESIGN ANALYSIS

It is well known that dipole antennas need balanced feeding such as using parallel dual-line transmission lines. However, microstrip lines commonly utilized in RF & microwave circuits are of the unbalanced type. Thus, a printed unbalanced-balanced transformer, i.e., a microstrip balun [7–9], needs to be adopted for a printed dipole antenna. Fig. 1(a) shows the standard realization of the balun, which is composed of the conductive patterns on the top and bottom copper-foil layers and the middle dielectric layer. A metallized via-hole is formed to connect the two copper-foil layers. The exciting signal is fed into the microstrip line having a characteristic impedance of  $Z_m$  from the position of A on the top layer. Then the signal propagates to the bottom layer through the via-hole on the position of B. On the

bottom layer, a segment of parallel dual-line transmission line having a characteristic impedance of  $Z_p$  and a length of one-fourth wavelength, i.e.,  $\lambda_0/4$ , is connected to the ground on the lower side and terminated to the balanced load  $Z_L$  on the upper side. We can notice that the currents on the microstrip line and the parallel line are on the contrary directions, which produces the odd-mode operating of the balun and accordingly realizes the balanced exciting to the dipole. Looking into the circuits from the position of B, we can get the equivalent circuit of the balun as illustrated in Fig. 1(b). Then, its input impedance can be given by [6]

$$Z_{in} = \frac{jZ_L Z_p \tan\left(\frac{\pi f}{2 f_0}\right)}{Z_L + jZ_p \tan\left(\frac{\pi f}{2 f_0}\right)} \quad (1)$$

where  $f$  and  $f_0$  denote the operation frequency and the resonant frequency, respectively. Here, let  $Z_m = Z_L$  and then we get that while  $Z_p \rightarrow \infty$ ,  $Z_{in} = Z_m$  for any  $f$ . Thus, if the terminated load takes a purely resistive impedance that is equal to the characteristic impedance of the microstrip line and the parallel dual-line transmission line is designed to have a very high characteristic impedance, we will be able to achieve good matching at the feeding position of A. However, it is well known that a dipole performs as a purely resistor only at the resonant frequency. Fortunately, we can optimize the design parameters to reduce its impedance varying slope and consequently broaden its operational bandwidth, which will be discussed in detail below.

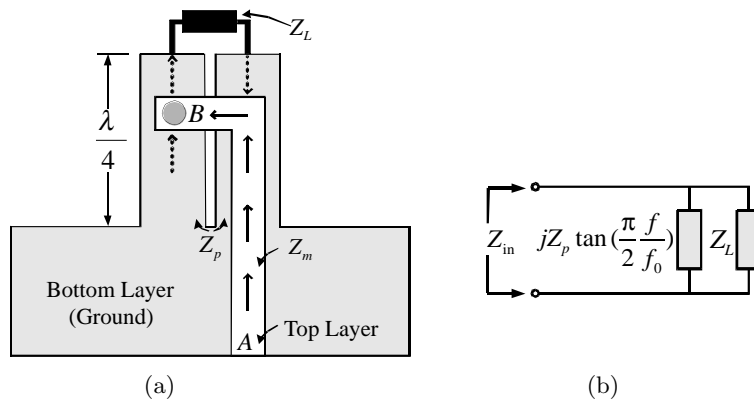


**Figure 1.** Printed microstrip balun. (a) Structure. (b) Equivalent circuit.

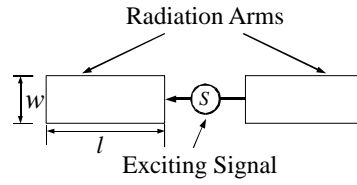


**Figure 2.** Standard realization of a printed dipole.

The standard realization of a printed dipole is illustrated in Fig. 2. For certain dielectric material, the length of the radiation arm dominates the resonant frequency and the width has a big effect on the impedance varying slope. It is well known that a printed dipole can be analyzed through treating it as an equivalent cylinder-type one that has a radius of  $r = w/4$  [10, 11]. Then, based on the formula presented in [6, 12], we can express its input impedance as

$$Z_{dipole} = \frac{120(\ln 8l - \ln w - 1)}{\cosh(2\alpha l) - \cos(2\beta l)} \left\{ \left[ \sinh(2\alpha l) - \frac{\alpha}{\beta} \sin(2\beta l) \right] - j \left[ \frac{\alpha}{\beta} \sinh(2\alpha l) + \sin(2\beta l) \right] \right\} \quad (2)$$

where  $\alpha$  and  $\beta$  denote the attenuation and phase-shifting coefficient of the dipole surface current. We can observe that while  $w$  is increased, the magnitude of the input impedance decreases and its slope also becomes flatter, which is advantageous to expanding the operating bandwidth. Thus,  $w$  should take as large a value as possible. Here, we design an dipole having the arm length of  $l \approx \lambda_0/4$ , the arm width of  $w \approx l/3$  and the resonant frequency of  $f_0 = 2.45$  GHz. The magnitude of its input impedance takes a value of  $50\Omega$ , which produces broad bandwidth and also facilitates to interconnecting with  $50\Omega$  coaxial cable and microstrip line popularly utilized in RF and microwave circuits. However, we must point out that while such a dipole is connected to the balun and the cable, the couplings between them will reduce the accuracy of (1) and (2). Since it is not easy to analyze these effects, we will make use of numerical simulations to optimize the practical design as shown in the later section.

Based on the research in [6], we also adopt a V-shaped ground plane to improve the antenna performance further. The ground at the feeding position of the microstrip line is extended and shaped as illustrated in Fig. 3. A sub-miniaturized A-type (SMA) connector is used to connect the feeding coaxial cable to the feeding point. The signal propagates towards the radiation arms via the microstrip

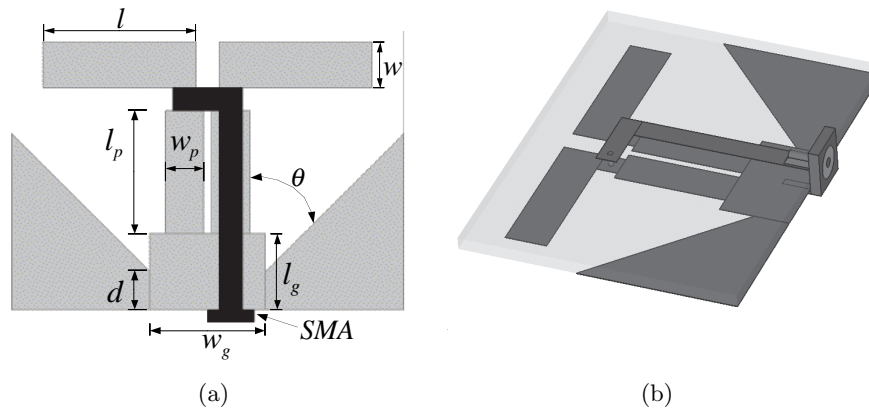


**Figure 3.** Structure of the printed dipole antenna with the V-shaped ground. (a) Top view. (b) Side view.

balun to realize the balanced exciting. The ground extends in the form of V shape towards the radiation arms, which efficiently reflects the electromagnetic waves towards the feeding direction to reduce the coupling between the dipole and the feeding cable and consequently improve the input voltage standing wave ratio (VSWR). If the extending angle  $\theta$  and position  $d$  of the ground have appropriate values, the reflected waves add up to the radiated waves, which gives rise to directive gain. The V-shaped structure also helps to broaden the operational bandwidth because the phase relations between the reflected and radiated waves do not change too much while the operational frequency is off the resonant frequency. Then, we utilize the FR-4 laminated board to design the antenna. The thickness of the copper layer is  $18\ \mu\text{m}$ , the thickness of the dielectric layer is  $1.6\ \text{mm}$ , the dielectric constant  $\epsilon_r$  is 4.6, and the tangent of the loss angle  $\delta$  is 0.018. Referring to Fig. 3, the antenna's dimensions are chosen as follows:  $l = 19\ \text{mm}$ ,  $l_p = 16\ \text{mm}$ ,  $l_g = 10\ \text{mm}$ ,  $w = 6\ \text{mm}$ ,  $w_p = 5\ \text{mm}$  and  $w_g = 15\ \text{mm}$ .

### 3. DESIGN OPTIMIZATIONS

We utilize the finite difference time domain (FDTD) 3D Electromagnetic simulations to characterize the antenna performance. The effects of the extending angle  $\theta$  and position  $d$  of the ground are investigated in order to obtain optimized design parameters.

Firstly, fixing  $d = 5\ \text{mm}$ , we vary  $\theta$  to study the variance of the

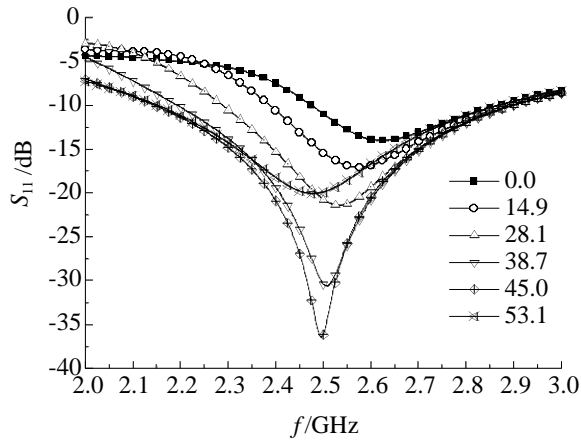


**Figure 4.** Input return loss ( $S_{11}$ ) of the antenna for different values of  $\theta$ .

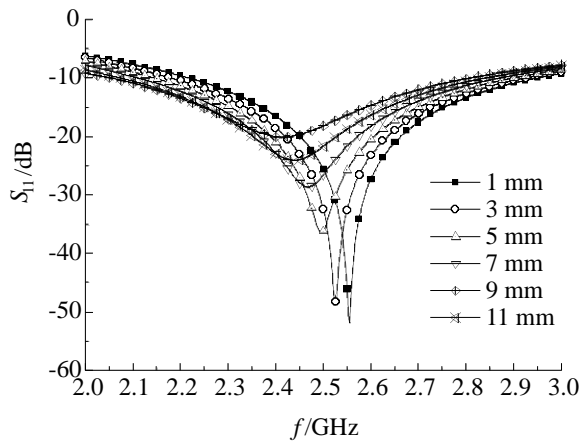


**Figure 5.** Input return loss ( $S_{11}$ ) of the antenna for different values of  $d$ .

input return loss  $S_{11}$ . The simulation results are shown in Fig. 4. It is observed that while  $\theta$  is equal to  $45^\circ$ , the antenna has good matching within a wide frequency band. Thus, we chose  $\theta = 45^\circ$ . Then, we fix  $\theta = 45^\circ$  and vary  $d$  to study the variance of the  $S_{11}$ . The simulation results are shown in Fig. 5. It is observed that while the ground is far away from the radiation arms, the matching becomes better due to the smaller capacitive loading on the dipole and simultaneously the resonant frequency becomes higher, which need to be mended through

lengthening the arm length  $l$ . To make a compromise between the matching and the size, we chose  $d = 5$  mm and then adjust  $l = 19.3$  mm to make the antenna operate at the center frequency of 2.45 GHz. A fabricated antenna based on the above design is illustrated in Fig. 6.

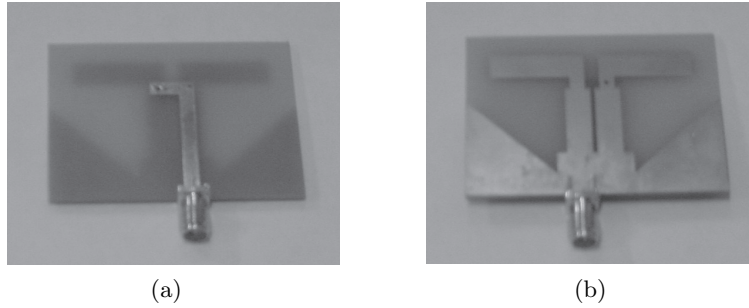


**Figure 6.** Photos of the fabricated antenna. (a) Top view. (b) Bottom view.

#### 4. MEASURED RESULTS

We measured the proposed antenna in a microwave anechoic chamber. The measured  $S_{11}$  and the voltage standing wave ratio (VSWR) are shown together in Fig. 7. Compared with the results presented in Fig. 4 of [7], we can observe that the operational bandwidth is improved by 5% and the matching also becomes better. Fig. 8 show the measured radiation patterns in  $H$  and  $E$  planes of the antenna at

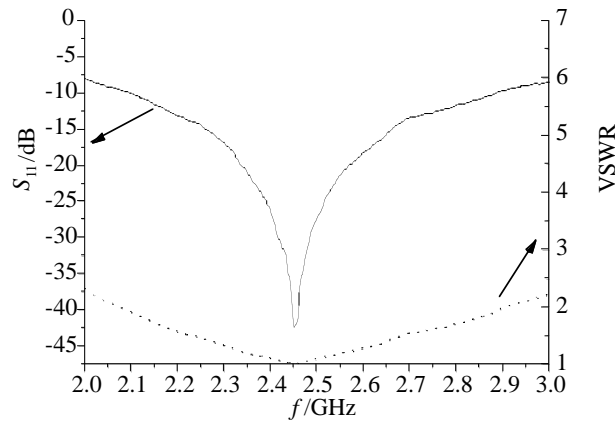
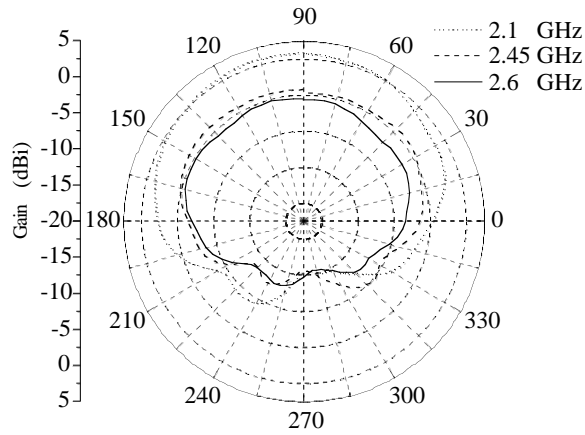
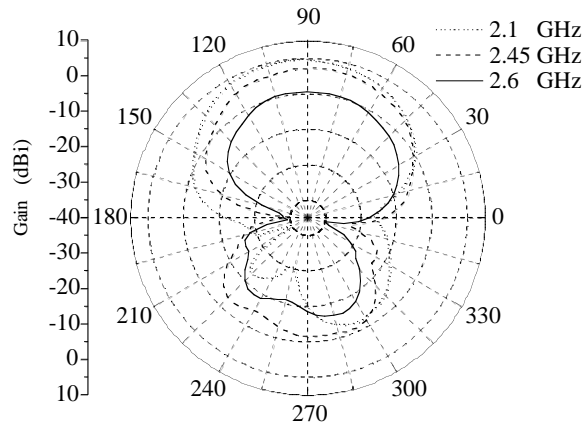


**Figure 7.** Measured input return loss ( $S_{11}$ ) and voltage standing wave ratio (VSWR) of the proposed antenna.

the frequencies of 2.1 GHz, 2.45 GHz and 2.6 GHz. Compared with the results presented in Fig. 6 of [7], we can see that the proposed antenna achieves certain directivity gain and accordingly suppresses the backward radiation by more than 7 dB. In addition, the radiation patterns keep similar properties in the operational frequency band, which is an advantage for broad bandwidth applications.



(a)



(b)

**Figure 8.** Measured radiation patterns of the propose antenna at three frequencies. (a) *H*-plane. (b) *E*-plane.



## 5. CONCLUSION

In this paper, a miniaturized printed dipole antenna with the V-shaped ground is proposed for radio frequency identification (RFID) readers operating at the frequency of 2.45 GHz. The principles of the microstrip balun and printed dipole are analyzed and design considerations are formulated. Through extending and shaping the ground to reduce the coupling between the balun and the dipole, the antenna's impedance bandwidth is broadened and the antenna's radiation pattern is improved. The 3D FDTD simulations are carried out to evaluate the antenna's performance. The effects of the extending angle and position of the ground are investigated to obtain the optimized parameters. The antenna was fabricated and measured in a microwave anechoic chamber. The results show that the proposed antenna achieves a broader impedance bandwidth, a higher forward radiation gain and a stronger suppression to backward radiation compared with the one without such a ground.

## ACKNOWLEDGMENT

This paper is supported by ZJNSF R105253 and in part by NSFC 60671003, 60531020.

## REFERENCES

1. Mitilineos, S. A., S. C. A. Thomopoulos, and C. N. Capsalis, "Genetic design of dual-band, switched-beam dipole arrays, with elements failure correction, retaining constant excitation coefficients," *Journal of Electromagnetic Waves and Applications*, Vol. 20, No. 14, 1925–1942, 2006.
2. Lei, J., et al., "An omnidirectional printed dipole array antenna with shaped radiation pattern in the elevation plane," *Journal of Electromagnetic Waves and Applications*, Vol. 20, No. 14, 1955–1966, 2006.
3. Ayestaran, R. G., J. Laviada, and F. Las-Heras, "Synthesis of passive-dipole arrays with a genetic-neural hybrid method," *Journal of Electromagnetic Waves and Applications*, Vol. 20, No. 15, 2123–2135, 2006.
4. Fan, Z. G., et al., "Signal descriptions and formulations for long range UHF RFID readers," *Progress In Electromagnetics Research*, PIER 71, 109–127, 2007.

5. Fan, Z. G., L. X. Ran, and J. A. Kong, "Source pulse optimizations for UWB radio systems," *Journal of Electromagnetic Waves and Applications*, Vol. 20, No. 11, 1535–1550, 2006.
6. Fan, Z. G., L. X. Ran, and K. S. Chen, "Novel printed dipole antenna with reflecting structure of V-shaped ground plane," *Journal of Zhejiang University (Engineering Science)*, Vol. 39, No. 9, 1292–1295, 2005.
7. Chuang, H. R. and L. C. Kuo, "3-D FDTD design analysis of a 2.4-GHz polarization-diversity printed dipole antenna with integrated balun and polarization-switching circuit for WLAN and wireless communication applications," *IEEE Transactions on Microwave Theory and Techniques*, Vol. 51, No. 2, 374–381, 2003.
8. Baward, R. and J. J. Wolfe, "A printed circuit balun for use with spiral antennas," *IRE Transactions on Microwave Theory and Techniques*, Vol. 8, No. 3, 319–325, 1960.
9. Edward, D. and D. Rees, "A broadband printed dipole with integrated balun," *Microwave Journal*, No. 5, 339–344, 1987.
10. Butler, C. M., "A formulation of the finite-length narrow slot or strip equation," *IEEE Transactions on Antennas and Propagation*, Vol. 30, No. 6, 1254–1257, 1982.
11. Butler, C. M., "The equivalent radius of a narrow conducting strip," *IEEE Transactions on Antennas and Propagation*, Vol. 30, No. 4, 755–758, 1982.
12. Zhou, C. D., Y. K. Wang, and L. M. Zhou, *Theory and Engineering on Line Antennas*, 27–37, Xidian University Press, Xian, 1988.